Hydrol. Earth Syst. Sci. Discuss., 6, 3335–3357, 2009
www.hydrol-earth-syst-sci-discuss.net/6/3335/2009/

Hydrology and
Earth System
Sciences
Discussions

The snowmelt runoff forecasting model of coupling WRF and DHSVM

Q. Zhao[1,2], Z. Liu[2,3,4], M. Li[2,3], Z. Wei[2,3], and S. Fang[2,3]

[1]The States Key Laboratory of Cryospheric Sciences, Cold and Arid Regions Environmental and Engineering Research Institute, Chinese Academy of Sciences, Lanzhou, China
[2]College of Resources and Environment Science, Xinjiang University, Urumqi, China
[3]Oasis Ecology Key laboratory of Xinjiang Uygur Autonomous region, Xinjiang University, Urumqi, China
[4]International Center for Desert Affairs-Research on Sustainable Development in Arid and Semi-arid Lands, Urumqi, China

Received: 21 March 2009 – Accepted: 12 April 2009 – Published: 22 April 2009

Correspondence to: Q. Zhao (dsslab@163.com)

Published by Copernicus Publications on behalf of the European Geosciences Union.

Abstract

This study used the Weather Research and Forecasting (WRF) modeling system and the Distributed Hydrology-Soil-Vegetation Model (DHSVM) to forecast the snowmelt runoff in the 800 km^2 Juntanghu watershed of the northern slope of Tianshan Mountains from 29 February–6 March 2008. This paper made an exploration for snowmelt runoff forecasting model combing closely practical application in meso-microscale. It included: (1) A limited-region 24-h Numeric Weather Forecasting System was established by using the new generation atmospheric model system WRF with the initial fields and lateral boundaries forced by Chinese T213L31 model. (2) The DHSVM hydrological model driven by WRF forecasts was used to predicate 24 h snowmelt runoff at the outlet of Juntanghu watershed. The forecasted result shows a good agreement with the observed data, and the average absolute relative error of maximum runoff simulation result is less than 15%. The result demonstrates the potential of using meso-microscale snowmelt runoff forecasting model for flood forecast. The model can provide a longer forecast period compared to traditional models such as those based on rain gauges, statistical forecast.

1 Introduction

In some high-altitude mountainous areas of western China, snowmelt water is an important water resource and plays a vital role in reasonable use of water resources. To reservoirs and water power stations, snowmelt water is a primary storing source and plays an important part in controlling the quantity of water in the reservoirs and arranges the water used in industry, agriculture and living. Snowmelt water can ease drought in the semiarid and arid areas, but there will be a flood disaster if the snowmelt water melt rapidly causing spring snowmelt floods (Qiudong Zhao, 2007).

Research shows that since the 1980s, snowmelt flood amounts and frequency have been increasing on northern slope of Tianshan Mountains Region. The frequency of snowmelt flood in the 1990s increased 3 times as compared with that in the 1950s, causing serious damage to the national economical construction, as well as to the arable land and properties in the region (WU Su-fen, 2003; Li Yan, 2003). As populations continue to grow, the need for accurate forecasting of flood events becomes increasingly important.

Traditional flood forecasting models use observed meteorological data, so that the forecast period is dependent on the flood routing in a watershed, often only predicting floods several hours (beforehand). However, for flood warnings, we hope to have a longer forecast period, preferably 1–3 day. High resolution atmospheric models in limited areas offer promising accurate regional forecasts of meteorological fields when forced with realistic large-scale conditions. Recent work on the coupling of these atmospheric models with hydrological models has shown that the forecasting meteorological fields can be used to drive hydrological models to produce hydrographs at selected outlets. The forecast period can thus be extended compared to more traditional methods.

Atmospheric models have been used previously to force hydrological models for short-term flood prediction. For example, Miller and Kim (1996) coupled the Mesoscale Atmospheric Simulation model with the distributed hydrological model “TOPMODEL” to simulate a 1995 flooding event on the flood-prone Russian River of northern California. Andenson (2002), Lin (2002), Lu (2006) adopted a one-way or two-way atmospheric and hydrological coupling model to forecast the rainstorm floods and lengthen the flood predictable time successfully. Kenneth (2001) used the Atmospheric Research Mesoscale Model (MM5) and the Distributed Hydrology–Soil–Vegetation Model (DHSVM) to simulate a complex rain-on-snow flood event.

This paper focuses on the direct forecasts of 24 h high-resolution mesoscale Weather Research and Forecasting (WRF) to drive a distributed hydrological model (DHSVM) for the prediction of the amount of snowmelt runoff. Furthermore, the snowmelt runoff forecasting model was assessed by making a comparative result analysis between forecasted data and observed data.

2 Brief description of two models

2.1 Atmospheric model: WRF

The Weather Research and Forecasting (WRF) modeling system is a next-generation mesoscale modeling system (Michalakes et al., 2001; Wang et al., 2004; Skamarock et al., 2005) that serves both operational and research communities. It is designed to be a flexible, state-of-the-art atmospheric simulation system that is portable and efficient on available parallel computing platforms. WRF is suitable for use in a broad range of applications across scales ranging from meters to thousands of kilometers.

The system consists of multiple dynamical cores, preprocessors for producing initial and lateral boundary conditions for simulations, and a three-dimensional variational data assimilation (3DVAR) system. WRF is built using software tools to enable extensibility and efficient computational parallelism. The use of WRF system has been reported in a variety of areas including storm prediction and research, air-quality modeling, wildfire, hurricane, tropical storm prediction, and regional climate and weather prediction.

The key component of the WRF-model is the Advanced Research WRF (ARW) dynamic solver. The model uses terrain-following, hydrostatic-pressure vertical coordinate with the top of the model being a constant pressure surface. The horizontal grid is the Arakawa-C grid. The time integration scheme in the model uses the third-order Runge-Kutta scheme, and the spatial discretization employs 2nd to 6th order schemes. The model supports both idealized and real-data applications with various lateral boundary condition options. The model also supports one-way, two-way and moving nest options. It runs on single-processor, shared- and distributed-memory computers.

2.2 Hydrological model: DHSVM

The Distributed Hydrology–Soil–Vegetation Model (DHSVM) is a physically based, distributed hydrological model developed for use in complex terrain (Wigmosta et al., 1994). The model accounts explicitly for the spatial distribution of land-surface process, and can be applied over a range of scale, from plot to large watershed at subdaily to daily timescales.

The DHSVM model includes two-layer canopy model for evapotranspiration, an energy balance model for snow accumulation and melting, a two-layer rooting zone model and a saturated subsurface flow model. Digital elevation data are used to model topographic controls on incoming shortwave radiation, precipitation, air temperature, downslope surface water and soil moisture movement. At each time step the model provides a simultaneous solution to the energy and water balance equations for every grid cell in the watershed. Individual grid cells are hydrologically linked through a quasi-three-dimensional saturated subsurface transport scheme. The effects of topography on flow routing are obtained through the direct use of Digital elevation model (DEM) data. Each grid cell can exchange water with its eight adjacent neighbors. Local hydraulic gradients are approximated by ground surface slope (kinematic approximation). Thus a given grid cell will receive water from its upslope neighbors and discharge to its downslope.

Water confluence processes in DHSVM involve three parts: surface slope flow, road/route flow and soil moisture flow. Surface slope flow is the downslope surface runoff flow after evapotranspiration, infiltration vertically and the evaporation and infiltration will continue along the flow route during the flow process. Road/route flow occurs when the land surface category is road or route. The surface water evaporate upward only in the vertical direction. There is no infiltration downward. Soil moisture flow is water lateral flow in soil layer, in which soil horizontal diffusion is accounted.

3 Study area and parameter

3.1 Juntanghu Watershed: the study area

The Juntanghu River, located on the northern slope on Tianshan Mountains, Xinjiang China, (Fig. 1), is a small river, originating from the Tenniscar Glacier, beginning with the Terssi. According to the statistical analysis by Geographic Information System (GIS), the elevation of the headstream is approximately 3400 m, and the main part is between 1000 m and 1500 m. Streams join together at Mazal which is located in the middle reach of Juntanghu River where flow gathers together into the Red-Mountain Reservoir at the outlet of mountain area and then enters into plain area.

The catchment area is approximately 800 km^2, the length is 45 km, the average elevation is approximately 1500 m, the slope of the upriver is 62.5‰, and the slope of downstream is 52.6‰. The average annual runoff of this basin is approximately 3.89×10^8 m^3. The watershed has some obvious hydrological characteristics of an arid area river, and it can be divided into a runoff forming region and a runoff dissipate region, with a boundary at the outlet of mountain area. One reason for choosing this basin as our typical study area is that it is relatively small with a close hydrological circumscription, and that the snowmelt flood damage in the watershed is serious.

3.2 A limited-region 24-h numeric weather forecasting system

Today every Chinese meteorological station and meteorological service system can access the fourth-generation medium-term global numerical weather prediction system T213L31 forecast of the Chinese National Weather Service. In this paper, the T213L31 provided at 00:00 as the initial fields and lateral boundaries of WRF v2.2, of which the forecast period is 144 h, from 0 to 72 h with 3 h interval and 72 to 144 h with 12 h interval.

The Numeric Weather Forecasting System was run for 24-h meteorological forecast everyday.

3.2.1 Numerical experimental plan

The basic parameter of stimulated area

The central longitude and latitude was 86.5° E and 44.0° N. The horizontal resolution was 1 km and the grid numbers in North-South direction and East-West direction were 130 and 121, respectively. There were 18 layers of vertical direction. The total stimulated time length was 24 h with a time step of 3 s. A forecast of meteorological fields was outputted every hour.

The terrestrial data

The data included terrain elevation, land-use/vegetation, land-water mask, soil type, vegetation fraction and deep soil temperature from USA AVHRR satellite inversion data. The soil class was based on USDA texture, the terrain elevation was Global 30 s DEM data, and the vegetation category was USGS standard.

The physical process options

There were many physical process options in WRF for every parameterization scheme. Here, the schemes were selected, respectively as follows: The cumulus parameterization was New Kain-Fritsch scheme. The microphysics scheme was WRF Single-Moment 3-class scheme (WSM3). A rapid and accurate radiative transfer model (RRTM) longwave scheme and Dudhia scheme were adopted for long-wave radiation and short-wave radiation. The planetary boundary layer scheme was Yonsei University (YSU) scheme. The 5-layer thermal diffusion surface physics scheme was chosen.

3.2.2 The data-processing of meteorological fields

Temperature, humidity, wind speed, incident shortwave and longwave radiation, and surface pressure at 2 m were required by DHSVM. But humidity and wind speed could not be got directly from the WRF grid. But the wind speed filed of every sigma lever could be got from WRF model. In this study, the wind speed filed at the lowest sigma level was adopted instead of the wind speed at 2 m.The humidity can be calculated by water vapor mixing ratio and surface air pressure. The specific formula as follows:

$$e_s = 100 * [6.112 * \exp(17.67 * (t - 273.15)/(t - 29.65))] \tag{1}$$

$$\mathrm{rh} = 100 * \mathrm{qv}/[0.62197 * \mathrm{es}/(\mathrm{prs} - e_s)] \tag{2}$$

Where e_s is the saturation vapor pressure (Murry, 1967), t is temperature at 2 m; rh is humidity, qv is water vapor mixing ratio at 2 m, prs is surface pressure.

3.3 Hydrological model initialization

The DHSVM parameters can be broadly divided into two major steps. The first was to assemble surface characteristics data, including digital elevation data, soil characteristics, vegetation, snow data and stream network information. The model required attributes derivable from surface characteristics data for each model pixel. This step was facilitated by use of GIS, with appropriate overlays for each of the attributes. The second step was to assemble the model forcing data, which consists of time series of meteorological variables and spatial overlays used to distribute these forcing data, which were provided by the WRF model.

3.3.1 DEM

Elevation data taken directly from the DEM were used by DHSVM. Other topography attributes (like surface slope and drainage patterns) were derived from the DEM too. DEM for the catchment was obtained from the 1:50 000 contour map at 30 m spatial resolution. The DEM was then used to delineate the catchments. This procedure, which was implemented using an algorithm described by Jensen and Domingue (1998), is coded in most GIS programs, including Arc/INFO routing flow-direction. Additional processing was performed to preserve general flow characteristics.

3.3.2 Soils

The DHSVM soil data were based on three types of information: soil type, soil physical parameter (Lateral Conductivity, Exponential Decrease, Maximum Infiltration, Porosity, Bubbling Pressure, Field Capacity, Wilting Point, Bulk Density, etc.) and soil depth. The soil type data was taken directly from the Chinese 1:1 000 000 soil type classified map, which was interpolated at 30 m spatial resolution in Arc/INFO (Fig. 2). The soil physical parameters were defined according to the FAO global 17-catergory soil physical parameters data and the book “Soil in Xinjiang (1996)”. The soil depth data were calculated through defining the maximum soil depth (1.3 m) and the minimum soil depth (0.25) according to the filed observation based on DEM and program provided by Washington University.

3.3.3 Vegetation

Five Vegetation classes (grassland, farmland, water, bare land and even green needle leaf) were derived from Enhanced Thematic Mapper (ETM) classified satellite imagery (Fig. 3), and subsequently were processed to be similar in form to the data sets used by Kirschbaum (1997) and Matheussen, et al. (2000). In addition to land classification type, the DHSVM vegetation parameters (Height, Maximum Resistance, Minimum Resistance, Moisture Threshold, Vapor Pressure Deficit, Monthly leaf area index (LAI), Monthly Albedo, etc) were defined according to field observation and USGS 25-category vegetation physical parameters.

3.3.4 Snow information

The snow information was very important for stimulating snowmelt runoff, which the DHSVM model needed as an initial snow state file. The snow information included: snow cover and spatial distribution of snow water equivalent. In this paper, the EOS/MODIS data was used to get the snow cover information by a normalized difference snow index (NDSI):

$$\mathrm{NDSI} = (\mathrm{Ref}_4 - \mathrm{Ref}_6)/(\mathrm{Ref}_4 + \mathrm{Ref}_6) > 0.4\,, \quad \mathrm{Ref}_2 > 0.11 \tag{3}$$

Where Ref_2, Ref_4, Ref_6 is, respectively the reflectance of band 2, band 4 and band 6.

The spatial distribution of snow water equivalent was from the National Center for Atmospheric Research (NCAR) Final analysis data.

3.3.5 Stream network

The DHSVM stream network was based on three types of information: a mapping table which located a portion of a stream reaches within its appropriate grid cell and describes the depth, width, and aspect of the channel cut into the soil; a reach table described the length, slope, and class of a reach connected with the next reach downstream; and a class file with routing characteristics of width, depth, and roughness for each stream class. These files were derived from the DEM using an algorithm described by Wigmosta and Perkins (2001).

In essence, the DEM topology defines the stream locations, while the extent of the network is specified by the model user via a given support area (minimum area below which a stream channel is assumed to exist). For Juntanghu catchment, the contributing area is 324 000 m^2, which was based in part on field observations.

Stream order was defined for use in an initial classification of reaches into a manageable number of types to which channel characteristics could be indexed. Some manual adjustments based on limited field observation were conducted (Fig. 4). Class characteristics were defined according to field observations (where available) and the relative descriptive size of the classes. The channel depth, width, and roughness were imposed according to the reach classifications using GISWA algorithms (Wigmosta and Perkins, 1997). The average slope of each reach was calculated from the DEM.

4 The analysis

The time period for the case study was from 01:00 GMT 29 February 2008 to 00:00:00 GMT 6 March 2008.

4.1 The result analyses of forecasting meteorological fields

This study used the WRF with the initial fields and lateral boundaries provided by the T213L31 model to realize the 24 h-numerical weather forecast from 29 February 2008 to 6 March 2008. Figure 5 is the comparative map of observed meteorological data and corresponding grid forecasts.

From Fig. 5, we can see that: (1) there are certain deviations between forecasted and observed temperature in the highest and lowest points, the average error is 1.2 K. (2) The forecasted wind speed is higher than the observed data, because WRF only supplies wind speed in every sigma layer, where wind speed in the lowest sigma layer is adopted. But the wind speed is a relatively weak influence on the snowmelt runoff, and the error is just 1.54 m/s, so the forecasted data is acceptable. (3) The relative humidity forecasted deviation is larger when the humidity fluctuates significantly, but when the relative humidity is stable, the forecasted effect is better; the average error is 6%. (4) The forecasted results of solar radiation is generally good, observed data is significantly higher than forecasted data at midday when the water vapor is higher and the change of the clouds is more active as it is difficult to consider the effect of the clouds because of WRF low spatial resolution.

Overall these forecasting errors are relatively small, proving that limited regional numerical weather forecasting precision can meet the requirements of accurate snowmelt runoff forecasting.

4.2 The result analyses of snowmelt runoff

The DHSVM model was forced by forecasted meteorological fields at 1 km spatial resolution, but the DHSVM model is initialized at 30 m spatial resolution. So there is an interpolated program embedded within DHSVM model, which is based on the DEM data (30″) used by WRF model, the high-resolution DEM data (30 m) and temperature gradient.

Figure 6 shows the spatial change of snow water equivalent. Figure 7 is the comparative map of 24 h-forecasted discharge and observed discharge in outlet of Juntanghu basin from 29 February 2008 to 6 March 2008. The model efficiency coefficient and the relative error of maximum value are used to evaluate the effect of snowmelt runoff forecasting model. Table 1 is the test of runoff forecasted and observed results.

The model efficiency coefficient:

$$R^2 = \left[1 - \frac{\sum_{i=1}^{n} (Q_{\mathrm{obs}} - Q_{\mathrm{fore}})^2}{\sum_{i=1}^{n} (Q_{\mathrm{obs}} - \bar{Q}_{\mathrm{fore}})^2} \right] \times 100\% \tag{4}$$

Where Q_{obs} is the observed discharge, $\bar{Q}_{\mathrm{obs}}$ is the average observed discharge, is forecasted discharge.

The absolute relative error of maximum value:

$$R_m = \frac{Q_{\mathrm{obs},m} - Q_{\mathrm{fore},m}}{Q_{\mathrm{obs},m}} \tag{5}$$

Where $Q_{\mathrm{obs},m}$, $Q_{\mathrm{fore},m}$ is, respectively the observed and forecasted maximum discharge.

From Fig. 7 and Table 1, the following results were obtained: (1) the average efficiency coefficient is 0.8, which shows the forecasted data is in strong agreement with the observed data, and there is a same change trend in hydrological processes. (2) The maximum relative error of maximum data, which is very important for flood warning, is 13.2%. This means the snowmelt runoff forecasting model can meet the needs of snowmelt flood forecasting and flood warning.

5 Conclusions

Based on the latest development of atmospheric science and hydrology, according to the features of snowmelt flooding on northern slop of Tianshan Mountains, this study built a snowmelt runoff forecasting model coupling WRF and DHSVM, and verified the forecasted results. The conclusions are as follows: (1) The limited-region 24-h Numeric Weather Forecasting System was established by using the new generation atmospheric model system WRF2.2 with the initial fields and lateral boundaries provided by the T213L31. The weather predictions are in accord with observations on the whole. Good results were obtained. (2) The coupling of atmospheric and hydrologic models and a 24-h snowmelt runoff forecasting model was put forward through forecasted meteorological fields to force the DHSVM model. The simulated data showed strong agreement with the observed data, and the average absolute relative error of the maximum runoff in simulation is below 15%. The model realized the snowmelt runoff forecasting successfully.

This study provides safeguards for flood early warning systems, flood prevention disaster reduction, and water resources management by forecasting of the meso-microscale snowmelt runoff forecasting model. Coupling the atmospheric and hydrologic models can offer useful reference for hydrological forecasting and water resources management in the areas without observed data or data missing.

The result demonstrates the potential of using meso-microscale snowmelt runoff forecasting model for flood forecast. The model can provide a longer forecast period compared to traditional models such as those based on rain gauges, statistical forecast.

Acknowledgements. This work on meso-microscale snowmelt runoff-forecasting model is an important part of the Project of National Scientific Foundation of China “The decision support system of snowmelt flood warning of Xinjiang based on “3S” technology”.

The work was supported by a grant from the Major State Basic Research Development Program of China (973 Program) (No. 2007CB411502) and the National Scientific Foundation of China (Nos. 70361001 and 40871023).

References

Agricultural Bureau of Uygur Autonomus Region of Xinjiang, Soil Survey Office of Uygur Autonomus Region of Xinjiang: Soil in Xinjiang, Science Press, Beijing, 1996.

Anderson, M. L., Chen Z.-Q., Kawas, M. L., and Feldman M. L. A.: Coupling HEC-HMS with atmospheric models for prediction of watershed runoff, J. Hydrologic Engrg., 7(4), 312–318, 2002.

Jensen, S. K. and Domingue, J. O.: Extracting topographic structure from digital elevation data for geographic information system analysis, Photogramm. Eng. Remote Sens., 54(11), 1593–1600, 1988.

Kirschbaum, R. and Lettenmaier, D. P.: An evaluation of the effects of anthropogenic activity on streamflow in the Columbia River Basin, Washington, Water Resources Series, Technical Report, University of Washington, Seattle, p. 156, 1997.

Kenneth, J., Westrick and Clifford, F. Mass: An evaluation of a high-resolution hydrometeorological modeling system for prediction of a cool-season flood event in a coastal mountainous watershed, J. Hydrometeor., 2, 161–179, 2001.

Li, Y.: Change of river flood and disaster in Xinjiang during past 40 years, Journal of Glaciology and Geocryology, 25(03), 342–346, 2003.

Lin, C. A., Wen, L., and Béland, M.: A coupled atmospheric-hydrological modeling study of the 1996 Ha! Ha! River basin flash flood in Québec, Canada, Geophys. Res. Lett., 29(2), doi:10.1029/2001GL013827, 2002.

Lu G.-H., Wu Z.-Y., and Lei, W.: Application of a coupled atmospheric-hydrological modeling system to real-time flood forecast, Adv. Water Sci., 6, 847–852, 2006.

Matheussen, B., Kirshbaum, R. L., and Goodman, I. A.: Effects of land cover change on streamflow in the interior Columbia River Basin (USA and Canada), Hydrol. Process., 14, 867–885, 2000.

Michalakes, J., Chen, S., Dudhia, J., and Hart, L.: Development of a next generation regional weather research and forecast model. In: Developments in Teracomputing: Proceedings of the Ninth ECMWF Workshop on the use of high performance computing in meteorology, Singapore, 269–276, 2001.

Miller, N. L. and Kim, J.: Numerical prediction of precipitation and river flow over the Russian River watershed during the January 1995 storms, Bull. Amer. Meteor. Soc., 77, 101–105, 1996.

Title Page
Abstract | Introduction
Conclusions | References
Tables | Figures
◀◀ | ▶▶
◀ | ▶
Back | Close
Full Screen / Esc
Printer-friendly Version
Interactive Discussion

Murray, F. W.: On the computation of saturation vapor pressure, J. Appl. Meteorol., 6, 203–204, 1967.

Zhao, Q, Liu, Z., and Shi, Q.: EOS/MODIS data-based estimation of the daily snowmelt in Juntanghu Watershed, northern slope of Tianshan Mountain, in: Remote Sensing and Modeling of Ecosystems for Sustainability IV, Proc. of SPIE Vol. 6679, 66791C, doi:10.1117/12.732952, 2007.

Skamarock, W. C. and Klemp, J. B.: The stability of time-split numerical methods for the hydrostatic and the nonhydrostatic elastic equations, Mon. Wea. Rev., 120, 2109–2127, 1992.

Wang, W., Barker, D., Bruyere, C., Dudhia, J., Gill, D., and Michalakes, J.: WRF Version 2 modeling system user's guide: http://www.mmm.ucar.edu/wrf/users/docs/user_guide/UsersGuideV2.1.pdf, last access: 2005.

Wigmosta, M. S., Vail, L. W., and Lettenamaier D. P.: A distributed hydrological-vegetation model for complex terrain, Water Resour. Res., 30(6), 1665–1679, 1994.

Wigmosta, M. S. and Perkins, W. A.: A GIS-based modeling system for watershed analysis: Final Report to the National Council of Paper Industry for Arid and Stream Improvement, 1997.

Wigmosta M. S. and Perkins, W. A.: Simulating the effects of forest roads on watershed hydrology, In: Influence of Urban and Forest Land Use on the Hydrologic Geomorphic Responses of Watersheds, edited by: Wigmosta M. S., Burges S. J., AGU Water Science and Application Series, p. 2, 2001.

Wu, S.-F. and Zhang, G.-W.: Preliminary approach on the floods and their calamity changing tendency in Xinjiang region, Journal of Glaciology and Geocryology, 25(2), 199–203, 2003.

Table 1. The test of forecasted and observed results.

Index	Date					
	29.2.2008	1.3.2008	2.3.2008	3.3.2008	4.3.2008	5.3.2008
Efficiency coefficient	0.67	0.952	0.912	0.66	0.68	0.96
Relative error of maximum data	5.19%	2.97%	3.40%	13.2%	11.06%	8.65%

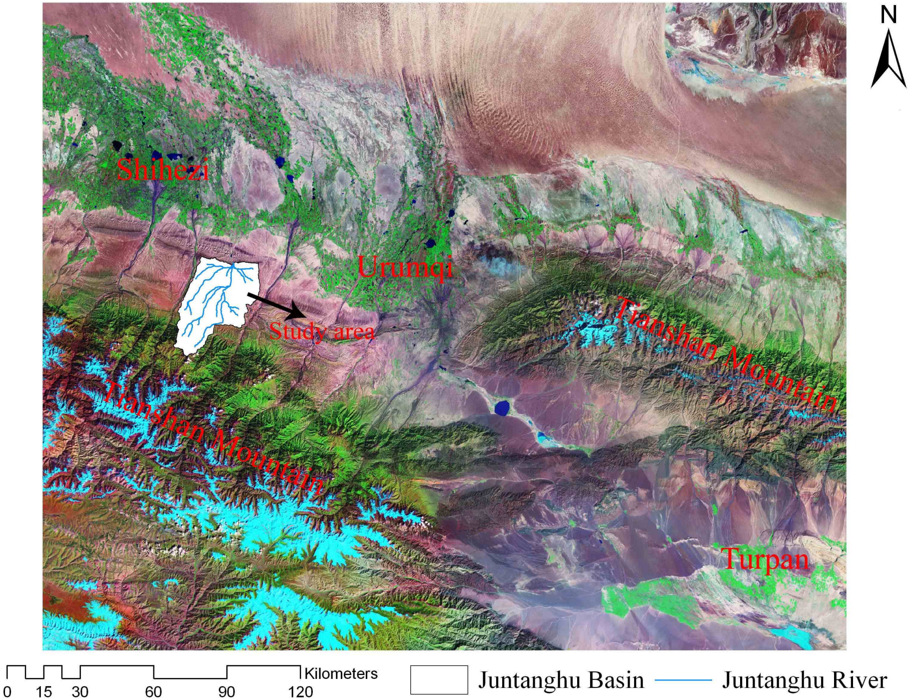

Fig. 1. The location of Juntanghu basin.

Title Page
Abstract
Introduction
Conclusions
References
Tables
Figures
◀
▶
Back
Close
Full Screen / Esc
Printer-friendly Version
Interactive Discussion

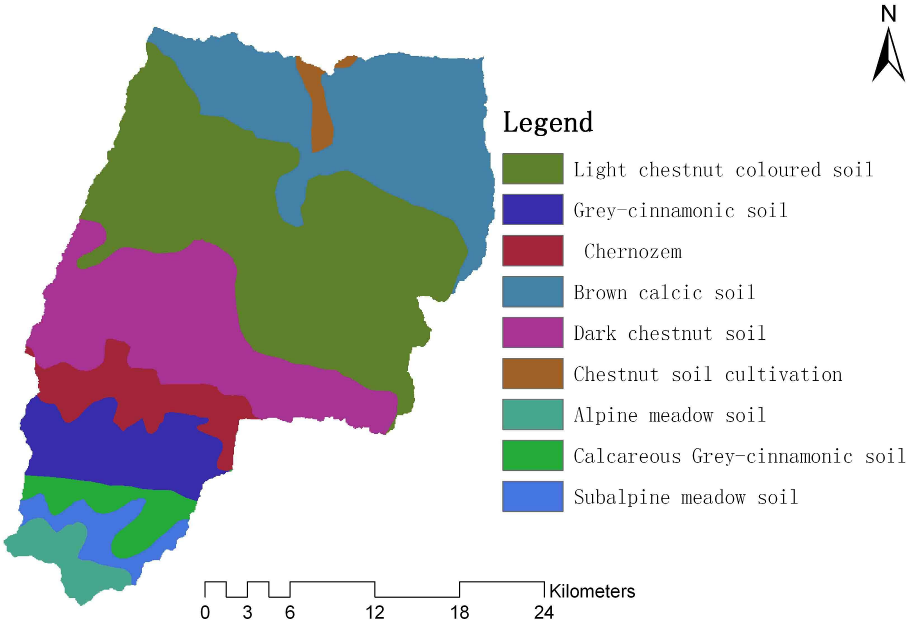

Fig. 2. The soil type map of study area.

Title Page
Abstract
Introduction
Conclusions
References
Tables
Figures
◀◀
▶▶
◀
▶
Back
Close
Full Screen / Esc
Printer-friendly Version
Interactive Discussion

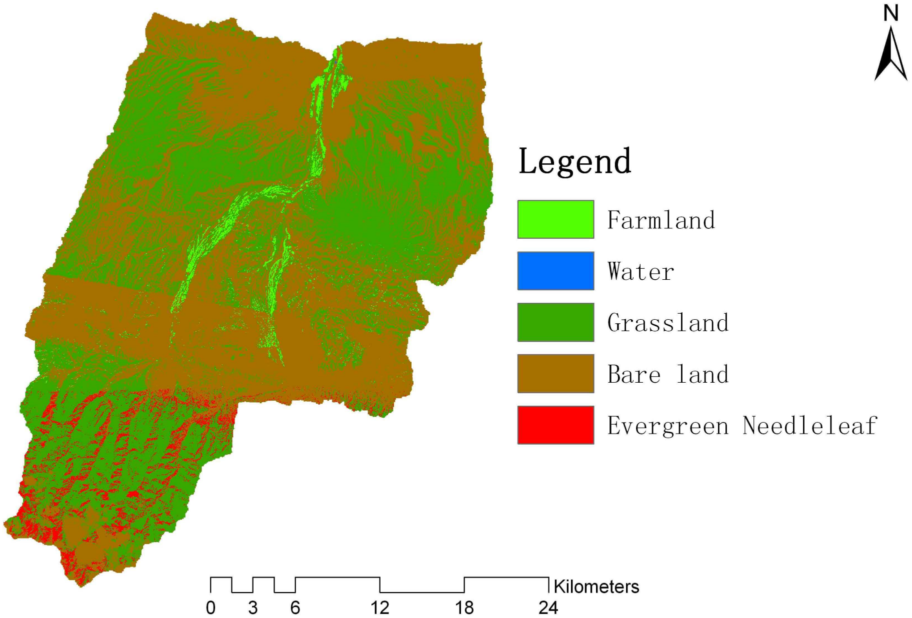

Fig. 3. The vegetation classification map of study area.

Title Page
Abstract | Introduction
Conclusions | References
Tables | Figures
◀| | |▶
◀ | ▶
Back | Close
Full Screen / Esc
Printer-friendly Version
Interactive Discussion

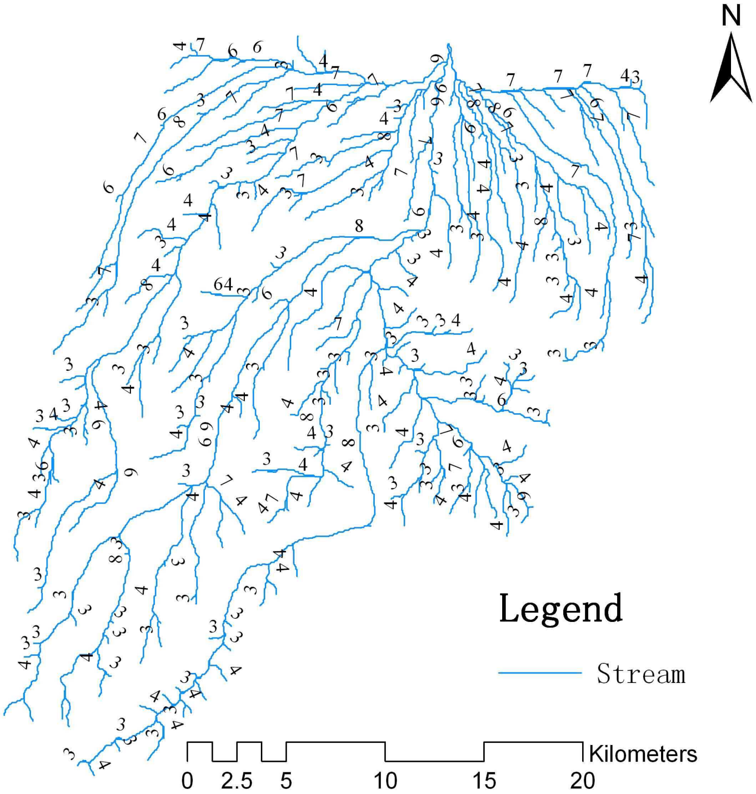

Fig. 4. The stream network of Juntanghu basin (the number is the stream order).

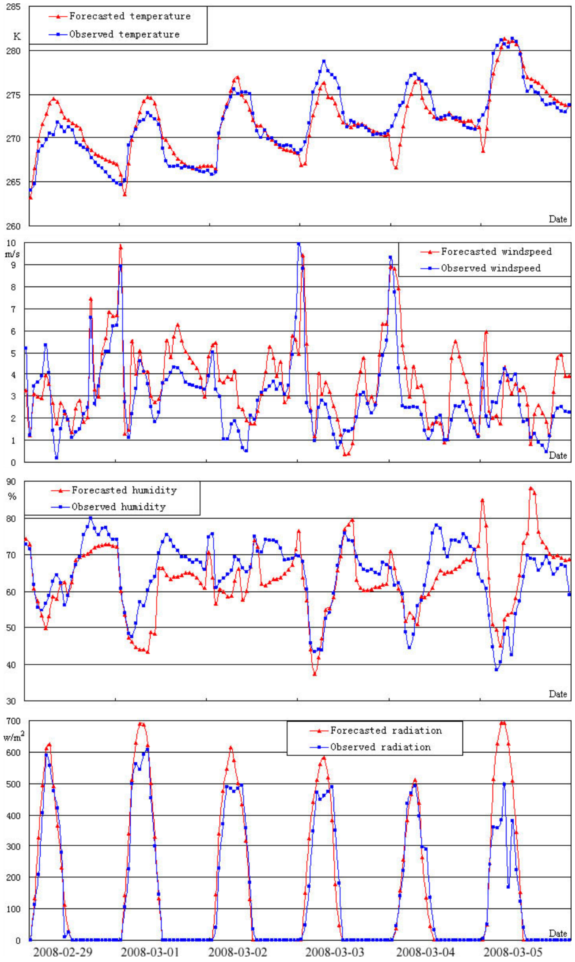

Fig. 5. The comparative map of forecasted meteorological data and observed data.

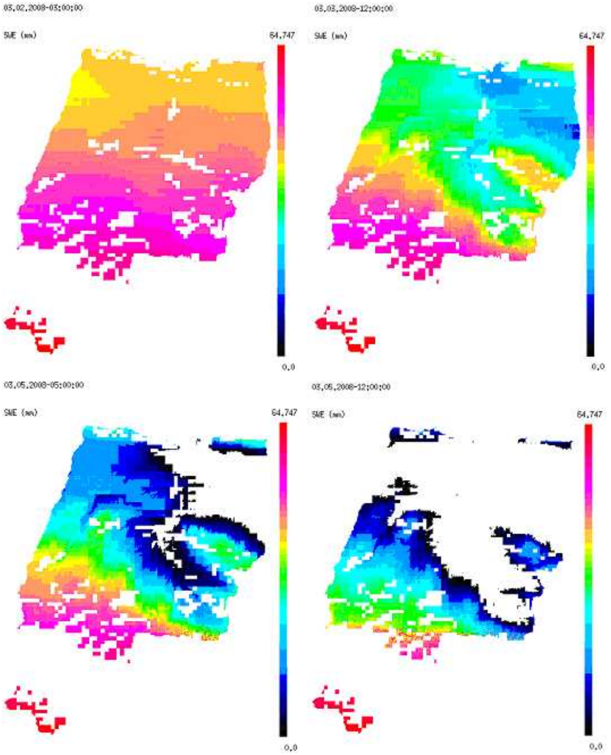

Fig. 6. The spatial change map of snow water equivalent.

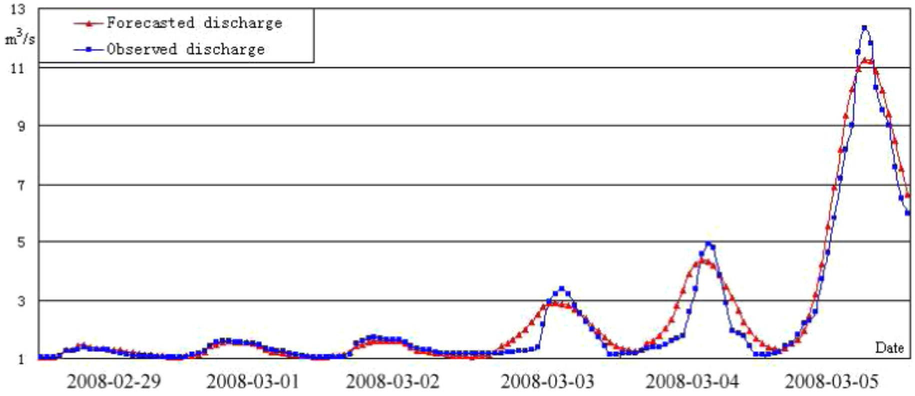

Fig. 7. The comparative map of forecasted discharge and observed discharge.